Exhibit 16

Environmental Science & Technology

Article

pubs.acs.org/est

Long-Term Changes in Sediment and Nutrient Delivery from Conowingo Dam to Chesapeake Bay: Effects of Reservoir Sedimentation

Qian Zhang,[*,†] Robert M. Hirsch,[‡] and William P. Ball[†,§]

[†]Johns Hopkins University, Department of Geography and Environmental Engineering, 3400 North Charles Street, Baltimore, Maryland 21218, United States

[‡]U.S. Geological Survey, 432 National Center, Reston, Virginia 20192, United States

[§]Chesapeake Research Consortium, 645 Contees Wharf Road, Edgewater, Maryland 21037, United States

Supporting Information

ABSTRACT: Reduction of suspended sediment (SS), total phosphorus (TP), and total nitrogen is an important focus for Chesapeake Bay watershed management. The Susquehanna River, the bay's largest tributary, has drawn attention because SS loads from behind Conowingo Dam (near the river's mouth) have been rising dramatically. To better understand these changes, we evaluated histories of concentration and loading (1986−2013) using data from sites above and below Conowingo Reservoir. First, observed concentration-discharge relationships show that SS and TP concentrations at the reservoir inlet have declined under most discharges in recent decades, but without corresponding declines at the outlet, implying recently diminished reservoir trapping. Second, best estimates of mass balance suggest decreasing net deposition of SS and TP in recent decades over a wide range of discharges, with cumulative mass generally dominated by the 75~99.5th percentile of daily Conowingo discharges. Finally, stationary models that better accommodate effects of riverflow variability also support the conclusion of diminished trapping of SS and TP under a range of discharges that includes those well below the literature-reported scour threshold. Overall, these findings suggest that decreased net deposition of SS and TP has occurred at subscour levels of discharge, which has significant implications for the Chesapeake Bay ecosystem.

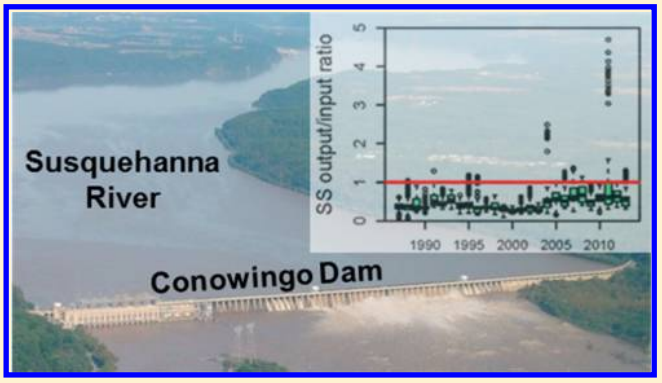

1. INTRODUCTION

To alleviate summertime hypoxia in Chesapeake Bay and associated impacts on estuarine ecology, reduction of nitrogen (N), phosphorus (P), and sediment loadings has been a long-term focus of Chesapeake Bay watershed management.[1−3] This endeavor has been recently reinforced with the promulgation of total maximum daily loads (TMDLs)[4] and state-wide efforts to establish watershed implementation plans.[5,6]

Among Chesapeake Bay's tributaries, Susquehanna River is the largest[1,3] and is one of nine that account for over 90% of nontidal discharge.[6] Of this 9-river non-tidal fraction, which has been modeled as accounting for ~77% of total freshwater discharge to the Bay (1991−2000; G. Shenk, personal communication),[6] the Susquehanna has contributed ~62% of flow, ~65% of total nitrogen (TN), ~46% of total phosphorus (TP), and ~41% of suspended sediment (SS), as based on measured flows and estimated loads over the period 1979 to 2012.[7] The relatively lower fractional contributions of TP and SS reflect retention within the Lower Susquehanna River Reservoir System (LSRRS), which consists of Lake Clarke (formed in 1931), Lake Aldred (formed in 1910), and Conowingo Reservoir (formed in 1928) (Figure 1).[8−10] In general, reservoirs in early stages of operation can effectively remove sediment and particulate P and N, mainly through particle deposition and burial,[11,12] and for N, possible denitrification.[13,14] Relative removal rates among constituents are also affected by escaping particles that are finer and therefore higher in P concentration than those retained[15,16] and by incoming N, which is predominantly dissolved and in contrast to P, which is predominantly bound to particles.[15,17,18] In this regard, estimates suggest that the LSRRS has historically trapped about 70%, 45%, and 2% of SS, TP, and TN loads, respectively.[19] Unfortunately, however, Lake Clarke and Lake Aldred have been effectively filled for several decades and the largest and most downstream reservoir, Conowingo, is reaching the end of its effective life for sediment removal,[8,9] as supported by a growing body of evidence documenting substantial recent

Received: August 21, 2015
Revised: January 6, 2016
Accepted: January 8, 2016
Published: January 8, 2016

DOI: 10.1021/acs.est.5b04073
Environ. Sci. Technol. 2016, 50, 1877−1886

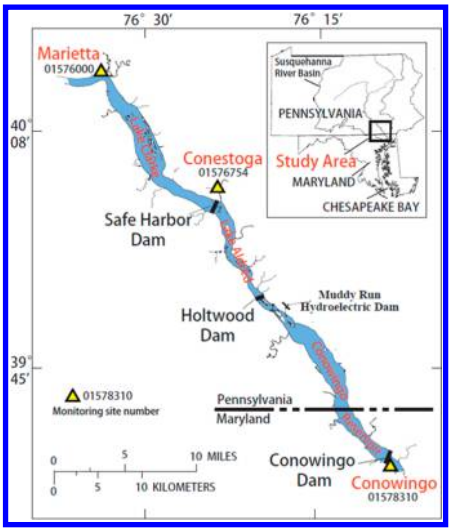

Figure 1. Map of the Lower Susquehanna River Reservoir System consisting of Lake Clarke, Lake Aldred, and Conowingo Reservoir. Yellow triangles indicate the three monitoring sites: Conowingo, Marietta, and Conestoga. (See SI Table S1 for site details.) This figure was modified after Figure 1 in Langland[8] with simplifications.

decline in net trapping of SS and particulate nutrients.[17,18] In this regard, statistical evaluations of trends for both dissolved and particulate species across the LSRRS have suggested that input loadings of all species have declined since the 1980s, but that output loadings of SS and particulate nutrients have trended upward since the mid-1990s.[18] Langland et al.[19] have estimated that once the Conowingo Reservoir reaches its sediment storage capacity and assuming no change in the inputs of SS and TP to the reservoir, average annual loads of SS and TP flowing past Conowingo Dam would increase by about 250% and 70%, respectively, as compared with loads observed before the reservoir neared its sediment storage capacity. In this context, a "SS scour threshold" of ~11 300 m^3/s (400 000 ft^3/s) was reported in 1978, which has likely decreased in more recent years.[20] As reservoir storage approaches capacity, there are remaining questions about the new "dynamic equilibrium" that will occur. In particular, little is known about the intra-annual phenology of sediment discharges, that is, the relative importance of increased magnitude and frequency of scour events at very high discharges and the decrease in sediment deposition during the much more frequent times of moderate to high discharges.

In the broader context of the nontidal Chesapeake watershed, recent work on its nine major tributaries has documented general rising trends in SS and particulate nutrient loads.[7] These trends are not well understood but may relate to (1) land-related practices such as land clearance and urbanization,[21,22] (2) removal of small mill dams,[23,24] and (3) increasing erosion of river bed and bank sediments,[22,25] particularly under the condition of increasing storm intensity.[26] Within this context, the Susquehanna rise was estimated to have contributed ~92% and ~68% to the total (nine non-tidal tributaries) summed rise of SS and TP, respectively, during the decade of 2002−2012.[7]

To provide new insights on sediment and nutrient processing within the LSRRS, we have further evaluated the history of concentration and loading from sites above and below the LSRRS for the period between 1986 and 2013 (~30 years) using available data from streamflow and concentration monitoring by the U.S. Geological Survey (USGS) and the Susquehanna River Basin Commission (SRBC). Specifically, we performed three types of analyses on SS, TP, and TN with increasing use of statistical modeling:

(1) Identification of changes in concentration-discharge relationships at sites above and below the reservoir using observed data—see Sections 2.1 and 3.1 for methods and results, respectively;
(2) Evaluation of net deposition in the reservoir system using mass-balance analysis based on best estimates of loadings—see Sections 2.2 and 3.2; and
(3) Analysis of the effects of sediment accumulation on reservoir performance by better accommodating effects of streamflow variability through the development of three different historical stationary models of the concentration relation to discharge and season—see Sections 2.3 and 3.3.

These analyses have been made possible by the decadal-scale historical output and input data and the recent development of statistical modeling approaches. To our knowledge, such mass-balance analyses of long-term sediment and nutrient accumulations have heretofore not been conducted on any major reservoir system that is similarly close to the end of its period of effective sediment trapping.

2. DATA AND METHODS

2.1. Study Sites and Data. The nontidal Susquehanna River Basin covers portions of New York, Pennsylvania, and Maryland. It comprises four physiographic provinces, namely, Appalachian Plateaus (58% of the area), Valley and Ridge (32%), Piedmont (9%), and Blue Ridge (1%).[7] Land uses in this watershed comprise forested (67%), agricultural (29%), urban (2%), and other (2%).[27]

There are three monitoring sites located in the vicinity of the LSRRS (Figure 1; Supporting Information (SI) Table S1 in Appendix A). The Conowingo site (drainage area: 70 189 km^2) at the system outlet is at Conowingo Dam, which is on Susquehanna's fall-line and about 10 miles from the river mouth at Havre de Grace, MD. This site has been monitored by the USGS since the 1970s and represents discharge from over 99% of the Susquehanna watershed.[28] Two upstream sites, Marietta and Conestoga, have been monitored by the USGS[29] for streamflow and by the SRBC[30] for water quality since the mid-1980s. The Marietta site (drainage area: 67 314 km^2) is on the mainstem and represents the majority (~96%) of the watershed represented by Conowingo. The Conestoga site (drainage area: 1217 km^2) monitors runoff from the small but heavily agricultural Conestoga tributary. At the three sites, annual average streamflow per unit area is comparable, with minimum values of 0.27−0.32 m/year and maximum values of 52−58 m/year (SI Table S1).

2.2. Analysis with Standard WRTDS Models. Selection of methods for estimating constituent concentration and loading based on low-frequency monitoring data has been an important area of hydrological research. Recently, Hirsch et al.[31] have developed a method called "Weighted Regressions on Time, Discharge, and Season" (WRTDS). WRTDS provides improvements over prior methods (e.g., ESTIMATOR[32]), because it does not rely on assumptions about homoscedasticity of model errors, constancy of seasonal trends in concentration, or a fixed concentration-flow relationship.[31] In regard to homoscedasticity, ESTIMATOR invokes an assumption of

DOI: 10.1021/acs.est.5b04073
Environ. Sci. Technol. 2016, 50, 1877−1886

constant residual error across all seasons and discharges and hence has a bias correction factor (BCF) that is also constant across all seasons and discharges. By contrast, WRTDS takes into account the substantial differences among these errors and the BCFs are calculated accordingly.[33,34] Consequently, WRTDS estimates can better represent the changing seasonal and flow-related patterns and are more resistant to the problem of load-estimation bias. WRTDS has been used in a wide range of regional to national water-quality studies.[7,17,18,31,33−35]

We have applied WRTDS to estimate concentrations and loads for every day in the record based on daily streamflow (Q) and more sparse concentration (C) data. WRTDS was implemented using the *R* package called EGRET (Exploration and Graphics for RivEr Trends).[35] For a particular site, such estimation is performed in four steps. First, WRTDS establishes a set of evenly spaced grid points on a surface defined by time (t) and log(Q). Grid values for the time and discharge dimensions were selected in accordance with a standard grid design described in the user manual (c.f. pages 40, 46−47).[35] Coarser and finer grid resolutions were tested during the development of the WRTDS model. Results were shown to be insensitive to resolutions finer than this standard grid design. Second, for each grid point, WRTDS develops a separate weighted-regression model using observed data and estimates C:

$$\ln(C) = \beta_0 + \beta_1 t + \beta_2 \ln(Q) + \beta_3 \sin(2\pi t) + \beta_4 \cos(2\pi t) + \varepsilon \quad (1)$$

where β_i are fitted coefficients and ε is the error term. With respect to the use of logarithm form for both C and Q, it has been well established that these variables generally follow log-normal distributions, for example,[36−38] and we have confirmed this for our data. More importantly, the residuals from this model, fitted to the log of concentration, generally approximate normal distributions quite well, with only limited exceptions at the extremes of the distributions (SI Figures S1−S3 in Appendix B-I). Step 2 thus results in an estimated concentration regression "surface" as functions of t and log(Q); see examples for Conowingo in SI Figure S4 (Appendix B-II). In Step 3, concentration for each day in the record is estimated using a bilinear interpolation of this surface, with proper accommodation of retransformation bias.[35] Finally, the estimated C is multiplied by daily Q to estimate daily loading. To alleviate potential edge effects for years near the start or end of the record, the updated EGRET package (version 2.2.0) was used in this work; see the user manual (c.f. pages 17−18, 41).[35]

For each of the three sites, we implemented the standard WRTDS model to produce daily "true-condition"[31] loading estimates for SS, TP, and TN, respectively. Residual analysis indicates that the residuals have no structural relationship with time, discharge, or season. (See SI Figures S5−S7 in Appendix B-II.) To obtain uncertainty estimates on daily and annual loadings for each species at each site, we have followed the method of Hirsch et al.[39] which involves resampling (with replacement) of the raw concentration data to obtain 100 realizations of representative data sets and associated WRTDS-based estimates of daily and annual loadings. Our approach is more fully described in Appendix B-III, which includes uncertainty results for annual loadings (SI Figure S8).

The loading estimates were then used for mass-balance analysis. Specifically, mass loading rates at Conowingo were used to represent reservoir output and those at Marietta and Conestoga were summed to represent the vast majority of reservoir input (97.6% of drainage area). Nonetheless, reservoir input was further adjusted by including an estimated contribution from the small unmonitored area above Conowingo and below Marietta and Conestoga. This estimate was made using Conestoga loadings and the appropriate drainage area ratio. Finally, output loads were subtracted from input loads to determine reservoir net deposition.

2.3. Analysis with Stationary WRTDS Models. Inter-annual comparisons of loading and net deposition based on standard WRTDS models are influenced by the particular time history of discharges that happened in a given year as well as the concentration regression surface (concentration as a function of time and discharge). To better isolate and reveal the changes that have occurred in the concentration regression surface (which we presume to reflect changes in reservoir system function), we developed three historical "stationary" WRTDS models. (See SI Figure S9 in Appendix B−IV.) The term "stationary" in our context means that a temporally invariant regression surface was assumed to be applicable over the entire period of record (i.e., a "stationary" probability function of concentration conditioned on discharge and season). By comparing results based on regression surfaces obtained from three decadally separated years, applied to the same streamflow record, we are able to isolate the effect of the change in the regression surface itself. Because all three histories developed use the exact same streamflow record, any observed differences should better represent fundamental differences in reservoir system function among the three selected years.

First, we selected three one-year-wide C versus t, log(Q) regression surfaces from the standard WRTDS model. For simplicity but without losing generality, we selected the 1990, 2000, and 2010 annual surfaces (SI Figure S9). Second, we separately repeated each of these 1-year surfaces to fill in the entire time-span to produce three different "stationary" surfaces for the entire record. Finally, these three period-of-record stationary surfaces were respectively used in conjunction with the actual history of daily discharge to estimate daily loadings, using the interpolation approach as described in Section 2.2. Note that the difference among the three stationary models is captured by the selected surfaces, which are considered to represent water-quality conditions at the study site in those selected years. We performed this stationary-model analysis on SS, TP, and TN at each of the three sites. To provide estimates of the uncertainty of these modeled results, we have resampled (with replacement) the raw concentration data ten times to obtain concentration data replicates and used each replicate to develop the three (i.e., 1990-, 2000-, and 2010-surface based) stationary models. The resulting range of load estimates forms uncertainty bands that are subsequently shown as dashed lines on plots. In addition, as with the standard WRTDS estimates, we have also conducted mass-balance analysis on the stationary-model estimates to evaluate net deposition.

3. RESULTS AND DISCUSSION

3.1. Temporal Changes in Concentration vs. Discharge Relationships. The manner in which nutrient and sediment concentrations vary with streamflow (i.e., C−Q relationships) reflect the relative role of dilution in comparison to mechanisms of dissolution, erosion, and transport[40−44] and temporal changes in such relationships can therefore be useful indicators of changes in system function. In this section, we

DOI: 10.1021/acs.est.5b04073
Environ. Sci. Technol. 2016, 50, 1877−1886

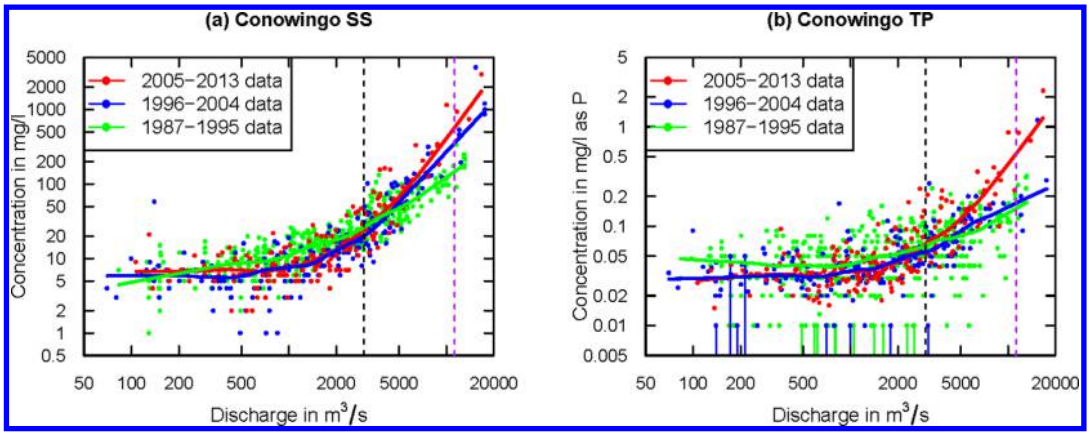

Figure 2. Observed concentration-discharge ($C-Q$) relationships for suspended sediment (SS) and total phosphorus (TP) in the Susquehanna River at Conowingo, MD, for three separate periods between 1987 and 2013. Solid lines are fitted LOWESS (locally weighted scatterplot smoothing) curves. Vertical black dashed lines in (a)−(b) correspond to 3000 m^3/s. Vertical purple dashed lines in (a)−(b) indicate the literature scour threshold of 11 300 m^3/s (400 000 ft^3/s). Data points with vertical solid lines in (b) indicate left-censored concentration samples. (Detection limit varied with samples.)

present an analysis of this type for the two mainstem sites: Conowingo (reservoir outlet) and Marietta (reservoir inlet). $C-Q$ scatterplots were constructed for three 9-year periods, 1987−1995 ("P_1"), 1996−2004 ("P_2"), and 2005−2013 ("P_3"), as shown in Figure 2 and SI Figure S10 of Appendix C. Nonparametric LOWESS (locally weighted scatterplot smoothing) curves are shown to better visualize the $C-Q$ relationships.

For SS, the $C-Q$ curves are generally convex upward. At Conowingo (Figure 2a), $C-Q$ relationships are similar among the three periods at low discharges (<3000 m^3/s), but the curves at higher discharges are clearly more elevated at later periods (i.e., P_2 and P_3). By contrast, the curves at Marietta (SI Figure S10b) show clear decline at later time (P_3) at low discharges (<3000 m^3/s) but negligible difference between P_2 and P_3 at higher discharges. For TP, the patterns are generally similar to SS (Figure 2b and SI Figure S10d). For TN, Conowingo shows similar $C-Q$ relationships among the three periods at most discharges, except that at the very high discharges (>7000 m^3/s) P_2 and P_3 show higher concentrations than P_1 (SI Figure S10e). At Marietta, P_3 shows lower concentrations than P_1 and P_2 at most discharges (SI Figure S10f).

Overall, the $C-Q$ relationships for Marietta show lower concentrations in SS, TP, and TN in P_3 than P_1 and P_2 at most discharges, suggesting decreased inputs of these constituents from various sources (e.g., agricultural, point, atmospheric, and stormwater sources).[18,27] Such promising changes at Marietta, however, have not been propagated across the reservoirs to emerge at Conowingo, where trends are reversed at high discharges. These results tend to corroborate previous reports of decreasing net trapping[8,17,18] and highlight the critical role of the reservoir for sediment and nutrient retention and storage.

3.2. Changes in Net Deposition: Analysis of Loads from Standard WRTDS Models. In this section, we present mass-balance analysis of loadings across the reservoir using estimates from *standard* WRTDS models to estimate changes in net deposition in the reservoir (Section 2.2). While these estimates are currently our best approximation of historical loadings and can provide useful indication of reservoir function, we remark that they are model outputs subject to limitations of sample availability and complications of interannual flow variability. In the latter regard, we also further analyze the results using *stationary* WRTDS models (Section 3.3).

3.2.1. Cumulative SS Deposition in the Reservoir. To consider recent sediment deposition rates in the context of the reservoir's ~85 years of service, we reconstructed a long-term record of cumulative deposition behind Conowingo Dam. Specifically, estimates of annual net deposition between 1987 and 2013 were obtained by applying mass-balance analysis on upstream and downstream estimates derived using the standard WRTDS models. These results were then interpreted on a storage-volume basis by assuming that the 2008 bathymetry-based estimate of sediment capacity[8] is correct. Our estimates of annual net deposition can then be used to estimate capacity in years before and after 2008 and these estimates can then be compared with other bathymetry data. The results are shown as green points in SI Figure S11 of Appendix D-I. The resulting curve is very consistent with the 1996 bathymetry result and close to the 1990 bathymetry result, giving us some confidence in the method for the pre-2008 period.

Based on this curve, cumulative deposition behind Conowingo Dam has followed a concave shape between 1987 and 2013, suggesting a declining rate of net deposition during this period. Taking the year 2000 as a dividing-point, the estimated average rate of net deposition was ~1.70×10^6 tons/year for 1987−2000 but only ~0.72×10^6 tons/year for 2000−2010. By contrast, the 1929−1987 average rate was ~2.24×10^6 tons/year, based on the 1987 estimate and the original storage capacity (SI Figure S11 and Table S2; Appendix D-I). Thus, the average rates during 1987−2000 and 2000−2010 are only 76% and 32%, respectively, of the 1929−1987 rate. Overall, these results strongly suggest that annual rates of deposition have decreased over time, particularly in recent years. These findings are consistent with the literature.[8,17,18]

It is noteworthy that the reconstructed curve from 2008 to 2011 (green points in SI Figure S11) did not match the 2011 bathymetry-based capacity, which was conducted immediately after Tropical Storm (TS) Lee.[45] In particular, bathymetry suggests continued net deposition between 2008 and 2011, whereas WRTDS results suggest net scour in 2011. This inconsistency may reflect inaccuracies in either type of measurement and perhaps relate to both underestimated input loadings owing to missed input sampling during three

DOI: 10.1021/acs.est.5b04073
Environ. Sci. Technol. 2016, 50, 1877−1886

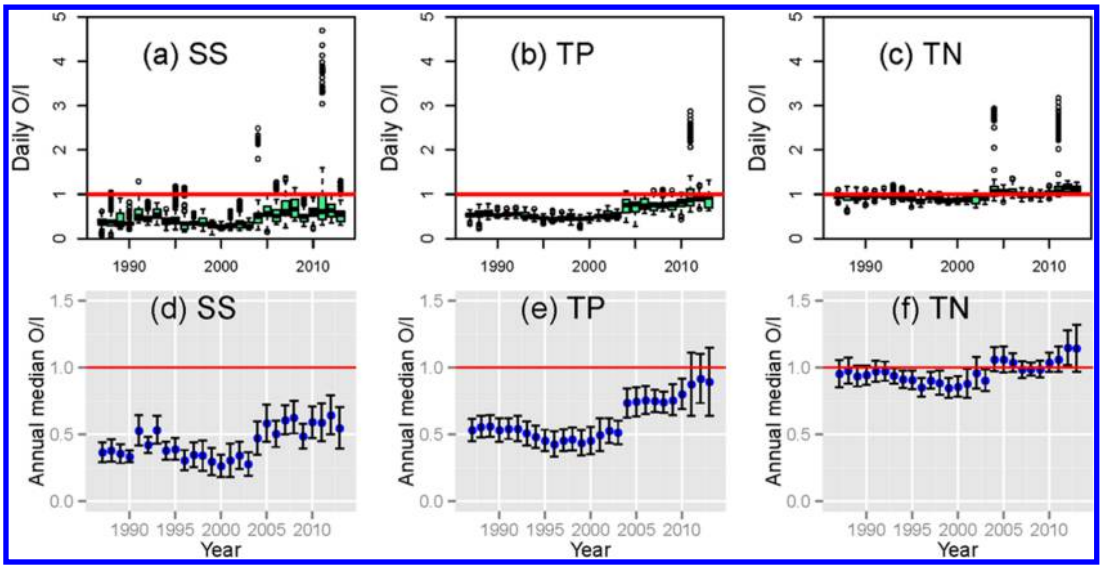

Figure 3. Estimated output/input ratios (O/I) based on 35 day moving averages of WRTDS-estimated output and input loadings. Plots (a)−(c) are annual boxplots for (a) suspended sediment (SS), (b) total phosphorus (TP), and (c) total nitrogen (TN). (Note that each boxplot represents 365 daily data points and that O/I < 1.0 reflects net deposition.) Plots (d)-(f) show the results of uncertainty analysis based on 100 synthetic data sets, see text. Plots show the averages of annual median values (blue dots) and the 95% confidence intervals (black error bars).

extremely highflow days in 2011 (i.e., September 8th, 9th, and 11th) and to overestimated output loadings at the high discharge end. Given the currently available data, we have conducted an uncertainty analysis to assign a 95% confidence interval on the cumulative deposition between 1987 and 2013, as shown with blue and purple points in SI Figure S11. This uncertainty interval increases dramatically during years of high flow such that it is able to capture the 2011 bathymetry as well as the earlier bathymetry results. In order to further examine the WRTDS results in the context of bathymetry, it is critical to conduct both new bathymetry surveys and continued monitoring of reservoir input and output, with more emphasis on fully capturing representative flow conditions.

3.2.2. Changes in Net Deposition over Time. To better understand decadal-scale changes in net deposition of sediment and nutrients, we quantified output/input ratios (O/I) for SS, TP, and TN and prepared boxplots of these ratios for each complete year (i.e., 1987−2013) (Figure 3). The ratios were calculated from 35-day moving averages of input and output loads to reflect travel time between Marietta and Conowingo. (Estimation of physical travel time in the LSRRS and rationalization of the selection of 35 days for the averaging period are described in Appendix D-II. This analysis reveals that the general trend is insensitive to averaging period for selections between 1 and 35 days; see SI Figures S12−S14.)

O/I results based on 35-day moving averages of input and output are provided in Figure 3, including both a single realization of WRTDS modeling of the original data (Figure 3a−c) and uncertainty analysis based on the 100 realizations obtained as described above (Section 2.2). Average annual median values of O/I, and their 95% confidence intervals, are shown in Figure 3d−f. Average numbers of excursions above 1.0, as well as their confidence intervals, are provided in SI Figure S15 (Appendix D-III).

In regard to SS and TP, Figure 3a−b reveal that annual median O/I has been rising, particularly since the 2000s. In addition, Figure 3d−e confirm that the trends in annual median O/I are qualitatively maintained based on the 100 realizations, but with overlapping confidence intervals. Figure 3a−b further reveal that annual 75th percentiles are approaching (SS) or exceeding (TP) 1.0, with substantial excursions in certain years (Figure 3a−b and SI Figure S15a−h). Overall, these results confirm the aforementioned trends of declining rate of net deposition. Given that streamflow O/I has been stable at ∼1.0 in 1987−2013 (not shown), these patterns in estimated SS and TP ratios most likely relate to diminished reservoir net trapping efficiency. The fact that TP ratios are generally greater than SS ratios suggests that decreasing retention in recent years is more pronounced for the finer (and more P-enriched) sediments, as should be expected since these fine sediments are more likely to be less well retained and more easily remobilized as reservoir infill continues.

In regard to TN, Figure 3c,f reveal that O/I has been generally stable with a median ∼1.0, but with a notable rise in recent years. Importantly, however, Figure 3c and SI Figure S15i−l also reveal substantial numbers of low-level excursions above 1.0, particularly in recent years. The different patterns in TP and TN O/I ratios reflect effective trapping of TP, which is dominated by PP, and generally inefficient removal of TN, which is dominated by dissolved N (DN) and particularly nitrate.[17−19] (Although removal of nitrate by algal growth and deposition might occur and some denitrification is possible, deposited particulate N [PN] can also be recycled as DN through bacterial activity in sediments.[13,14]) Although TN ratios are not far above 1.0 because of DN dominance, the annual numbers of excursion based on modeled estimates are actually much higher for TN than for SS and TP (SI Figure S15), possibly reflecting lower physical density and settling velocity for PN. In general, both the recent rise in TN O/I and the rising number of excursions above 1.0 reflect an increasingly larger quantity and fraction of PN in the reservoir output that deserves further study and management consideration.

One potential concern in regard to the ratio trends discussed above is that sampling dates varied between Marietta and Conowingo, with more highflow dates sampled at Conowingo, and that WRTDS surfaces may vary among sites in a way that could bias results. We examined the potential impact of this sampling issue by considering equally censored data at both

DOI: 10.1021/acs.est.5b04073
Environ. Sci. Technol. 2016, 50, 1877−1886

sites. (See details in Appendix D-IV and SI Figures S16–S18 therein.) Results show that our basic conclusions are unaffected by differences in sampling patterns (SI Figure S19).

3.2.3. Changes in Reservoir Trapping Efficiency as a Function of Flow. The above-noted changes in reservoir trapping have attracted considerable attention from managers and there has been a popular tendency to consider extreme storm events as the major concern for the future.[46] While extreme flows have indeed been important sources of sediment discharge, decreased net trapping by the reservoir is a more complex story that is relevant under many flow conditions. To better understand this problem, we evaluated sediment and nutrient loadings in five flow classes defined according to percentiles of daily Conowingo discharge, namely, Q_1 (0th to 25th percentile), Q_2 (25th to 50th), Q_3 (50th to 75th), Q_4 (75th to 99.5th), and Q_5 (99.5th to 100th). Note that Q_1 to Q_4 each contain ∼25% of the days in 1987–2013 but these flows are well below the literature-reported scour threshold of 11 300 m^3/s.[20] Q_5 contains the days with the 0.5% highest flows (50 out of 9862 days in the period of record), ranging from 7674 to 20 077 m^3/s, with the high end representing the highest daily discharge observed during TS Lee in 2011.

This flow-classified analysis reveals that SS and TP O/I ratios have increased since the early 2000s across all classes, as shown in SI Figures S20 and S21 (Appendix D–V), respectively, and despite the stable ∼1.0 ratio for flow. For TN, the general loading trends have been slightly downward for both input and output over the most record of 1987–2013 (SI Figure S22). TN O/I, however, has risen slightly since ∼2000 for Q_1–Q_4 and greatly for Q_5. The latter reflects the fact that PN losses have become much more significant in recent years, as confirmed through separate analysis of PN (data not shown). Because time averaging is not possible for flow-class data, daily based ratios are shown in SI Figures S20–S22. As previously noted, our comparative analysis suggests that these ratios also accurately reveal the broad trend in net deposition, despite the travel time issue.

In the above regard, it is noteworthy that Q_4 contains a large number of highflow days that, although well below the previously documented scour threshold, represent the highest cumulative discharge volume (V_w) and cumulative loading for almost all constituents for both reservoir input and output in 1987–2013 (Figure 4). For input (Figure 4a), Q_4 has contributed over half of V_w (55%), SS (64%), TP (59%), and TN (55%). For output (Figure 4b), Q_4 has contributed over half of V_w (54%), TN (53%), and TP (53%), although its SS contribution (35%) is less than Q_5 (58%) due to very high estimates of SS load for extremely highflow days that belong to Q_5. Interestingly, Q_5's contribution of SS at the outlet (58%) is much higher than that of TP (25%), owing to the facts that SS during high flows have a greater percentage of larger size fractions than at low flows and that larger particles have lower specific surface area and lower P:SS ratios. Nonetheless, our major conclusion from this analysis is that Q_4 has dominated the absolute mass of nutrient delivery and has contributed a major part of SS delivery through the reservoir, despite the fact that flows in Q_4 are generally insufficient to cause major scour.

3.3. Changes in Net Deposition: Analysis of Loads from Stationary WRTDS Models. In this section, we expand our analysis to consider cases where we force our WRTDS regression surfaces to be *stationary* (Section 2.3). The objective is to remove potential effects of interannual streamflow variability on the validity of our conclusions in regard to changes in reservoir trapping efficiency. For brevity, the 1990-, 2000-, and 2010-surface based stationary models are hereafter referred to as M_1, M_2, and M_3, respectively.

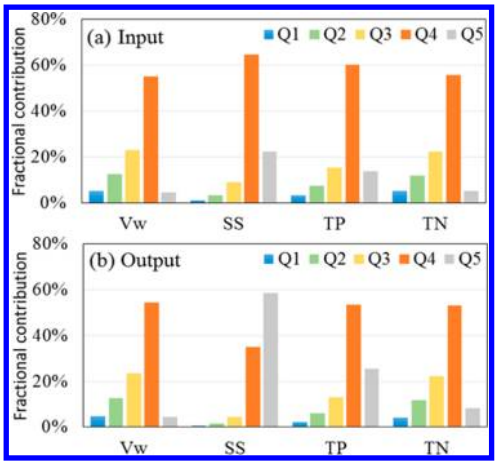

Figure 4. Fractional contribution of total streamflow volume (V_w) and nutrient and sediment mass discharges in the Susquehanna River at Conowingo by each of the five flow classes for reservoir input (a) and output (b) in 1987–2013. (Ranges of the five flow classes: Q_1: 25–396 m^3/s; Q_2: 399–787 m^3/s; Q_3: 790–1464 m^3/s; Q_4: 1467–7646 m^3/s; Q_5: 7674–20 077 m^3/s.).

3.3.1. Frequency Plots of Ranked Loadings. One way of comparing the three stationary models is to rank the estimated loadings and count the number of days per year that these loadings exceed certain values under each model. Such probability-of-exceedance plots are shown for all constituents at each count value (i.e., 0–365 days/year) in SI Figures S23–S31 of Appendix E–I. These figures also contain three enlarged portions for visual clarity, that is, 0–15, 100–115, and 200–215 days/year. For brevity, we focus on the beginning portion (i.e., the highest 15 days/year); these subplots are shown in Figure 5.

For SS at Conowingo (reservoir output), M_3 shows dramatically higher loading than M_1 and M_2 for the highest 15 days/year (Figure 5a). For example, Conowingo (reservoir outlet) SS loading is estimated to exceed 50 million kg/day with a frequency of 3, 4, and 7 days/year under M_1, M_2, and M_3, respectively. Moreover, the uncertainty bands of M_3 (shown as red dashed lines) are always above those of M_2 and M_1 (blue and green dashed lines), indicating that the noted rise with M_3 is robust. Further along the x-axis, M_3 becomes less distinguishable from M_1 and M_2 (SI Figure S23c,d). For Marietta (reservoir inlet), M_3 is always below M_1 and M_2 (Figure 5b and SI Figure S24), indicating declined loading based on the most recent watershed condition (2010) than prior conditions (1990 and 2000). These results are consistent with the aforementioned conclusion that upstream watershed load has declined even while outlet load has risen. For net rates of SS storage (i.e., net deposition), M_3 has evidently decreased in relative to M_1 and M_2 for the highest 15 days/year (Figure 5c). For instance, under M_1, SS net deposition exceeds 115 million kg/day with a frequency of 2 days/year. At this same frequency the net deposition exceeds 110 million kg/day under M_2 and 40 million kg/day under M_3. Further along the x-axis, the M_3 model also shows less net deposition than the other two models (SI Figure S25c,d).

Results for TP are generally similar to those of SS (Figure 5d–f). For example, Conowingo TP loading is estimated to

DOI: 10.1021/acs.est.5b04073
Environ. Sci. Technol. 2016, 50, 1877–1886

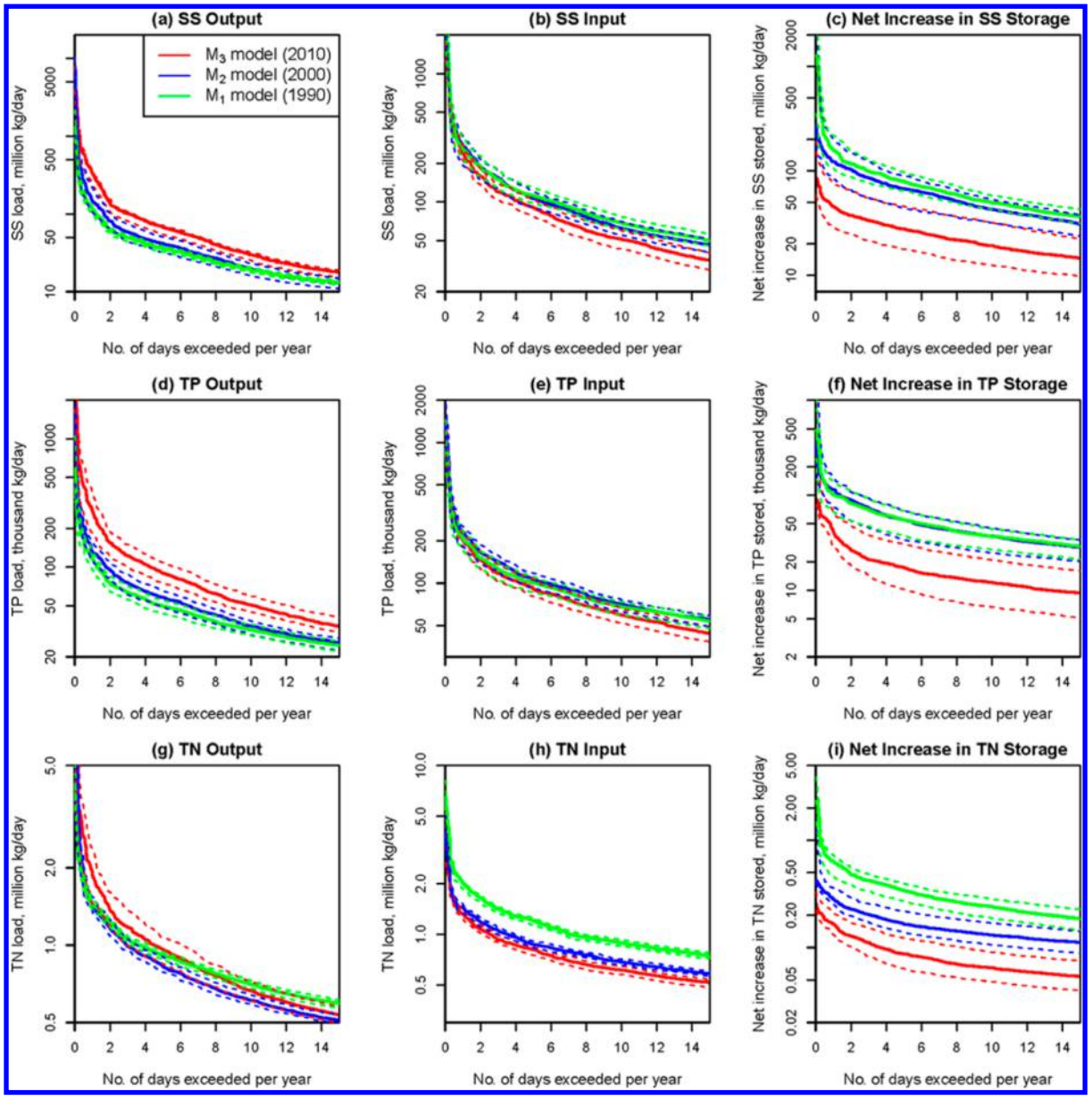

Figure 5. Frequency plots of ranked loadings for reservoir output, input, and net increase in storage for suspended sediment (SS), total phosphorus (TP), and total nitrogen (TN) based on the three historical stationary WRTDS models. For output (panels a, d, g) and input (panels b, e, h), dashed lines represent the upper and lower limits of model results derived from 10 replicates of each model that were based on resampled (with replacement) concentration data. For net increase in storage (panels c, f, i), dashed lines indicate the 95% confidence intervals based on 100 sets of net storage estimates obtained from the resulting 10×10 input × output matrix. See SI Figures S23–S31 in Appendix E–I for the full range of *x*-axis (i.e., 0–365 days/year).

exceed 50 000 kg/day on about 5 days/year under M_1, 6 days/year under M_2, and 10 days/year under M_3 (Figure 5d). For reservoir input, M_3 is always below M_1 and M_2 (Figure 5e and SI Figure S27), indicating decreased TP loading based on the most recent watershed condition (2010) than prior conditions. For TP net deposition, M_3 has evidently decreased in relative to M_1 and M_2 (Figure 5f). For instance, out of 2 days per year, net TP deposition exceeds 85 000 kg/day under M_1, 90 000 kg/day under M_2, but only 25 000 kg/day under M_3. Further along the *x*-axis, M_3 also shows less net deposition than the other two models (SI Figure S28c,d).

Results for TN do not follow those for SS and TP at Conowingo—the three models show generally similar loadings, except that M_3 is above M_1 and M_2 for the range of 0–6 days/year (Figure 5g). Further along the *x*-axis, M_3 and M_2 become indistinguishable but are both lower than M_1 (SI Figure S29c–d). For reservoir input, TN loading generally follows the pattern of $M_1 > M_2 > M_3$ (Figure 5h and SI Figure S30), suggesting recent TN load decline in the upstream watershed. For TN net deposition, the pattern is similar to that of SS or TP, with M_3 showing less net deposition than the other two models (Figure 5i and SI Figure S31c,d).

Overall, the stationary-model results are consistent with the other indications, suggesting that (1) reservoir inputs of SS, TP, and TN have generally declined, (2) reservoir outputs of SS and TP have increased, and (3) reservoir net deposition of SS and TP has declined considerably. Such estimates serve to better quantify changes in reservoir trapping capability and can

DOI: 10.1021/acs.est.5b04073
Environ. Sci. Technol. 2016, 50, 1877–1886

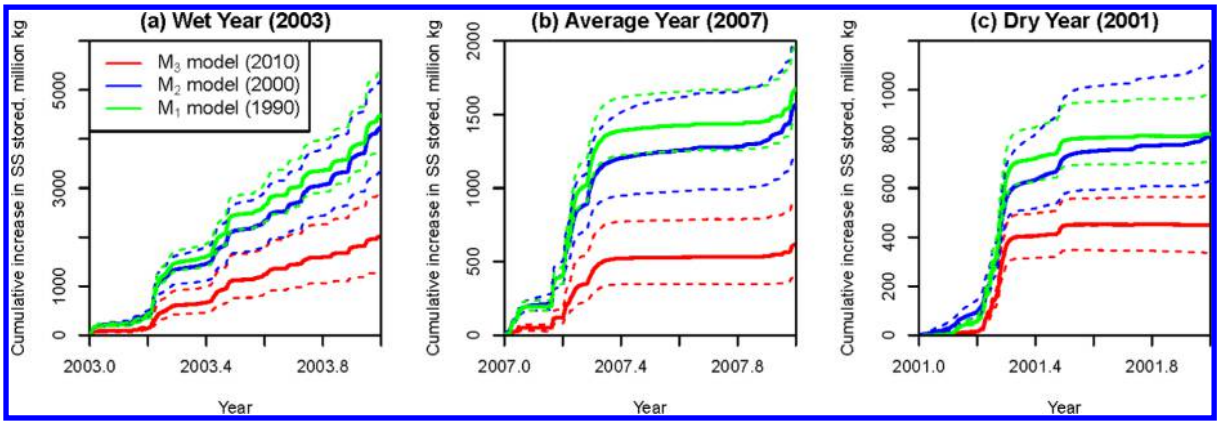

Figure 6. Modeled cumulative reservoir storage over the course of three selected wet, average, and dry calendar years (i.e., 2003, 2007, and 2001) with respect to suspended sediment (SS) loads based on the three stationary WRTDS models. Dashed lines represent the 95% confidence intervals based on 100 sets of net storage estimates obtained from a 10×10 matrix created from 10 replicate runs of each model at both the inlet and outlet and based on random resampling with replacement of observed concentration data. See SI Figure S41 in Appendix E-III for results on SS output and input loadings.

be useful to inform the refinement of Chesapeake Bay Watershed Model for purposes of Chesapeake Bay TMDL allocation.[5,6] Although this retrospective analysis does not speak to the issue of future conditions, it can serve to inform and constrain future analysis and modeling, which is a research topic of great importance to Chesapeake Bay restoration.

3.3.2. Changes in Reservoir Trapping Efficiency as a Function of Flow. As with the standard WRTDS analysis (Section 3.2.2), we find it useful to consider the stationary-model results in regard to the flow interval associated with major changes in reservoir function. Thus, we similarly evaluated loadings as a function of discharge for stationary-model estimates and fitted LOWESS curves to the modeled loading vs observed discharge. These plots are provided in SI Figures S32−S40 of Appendix E-II. Readers should appreciate that these statistically modeled loading-discharge relationships are highly uncertain at the highest discharges (i.e., those associated with infrequent weather-related events) due to the scarcity of concentration monitoring data at one or more locations during these discharges and the related fact that available measurements may not accurately represent the proper flow-weighted distribution of concentration. Although full discussion of this issue is beyond our current scope, we nonetheless caution against over-interpretation of model results at such extreme discharges. In our discussion below, we focus on the broader range of discharges where more data are available and with special focus on SS and TP because these constituents are most sensitive to reservoir trapping.

For SS at Conowingo (reservoir output), the M_3 curve is clearly above M_1 and M_2 for discharge above ~2500 m^3/s but less distinguishable at lower discharge (SI Figure S32). For reservoir input, however, differences among the three models are observed mainly for discharge below ~5000 m^3/s, with M_3 loading being the lowest (SI Figure S33). For reservoir net deposition, the M_3 curve is clearly below M_1 and M_2 for a wide range of discharges (> ~150 m^3/s) (SI Figure S34).

Results for TP are similar to those for SS, but with the clear separation of curves extending down to ~1700 m^3/s for Conowingo (SI Figure S35). And as with SS, input of TP under M_3 shows smaller loading than under M_1 and M_2 for discharge below ~5000 m^3/s (SI Figure S36). Finally, reservoir net deposition of TP is smaller under M_3 than M_1 and M_2 for the entire range of discharges (SI Figure S37).

Overall, these loading-discharge relationships confirm the previous finding (Section 3.2.3) that diminished reservoir trapping of SS and TP has occurred under a wide range of flow conditions, including flows well below the literature-reported scour threshold.[20] Therefore, even if future Conowingo discharge remains largely below this threshold, there will likely be continued decreased net trapping and increased loadings for SS and TP at Conowingo Dam. Moreover, these stationary-model results confirm that the observed changes could have occurred because of diminished reservoir trapping efficiency and there is no need to invoke climatic factors such as increased streamflow variability to explain the changes.

3.3.3. Cumulative Loading for Selected Representative Wet, Average, And Dry Years. The developed stationary models can also be used to explore estimated cumulative increases in storage (i.e., cumulative net deposition) for different types of hydrological conditions, that is, "wet," "average," and "dry" years. Toward that end, we have selected 2003, 2007, and 2001, as representative years for wet, average, and dry conditions, respectively. These years had average flows of 1718, 1009, and 667 m^3/s, and represent the 4th, 13th, and 27th highest-flow years, respectively, based on ranking of annual Conowingo streamflow between 1987 and 2013. We have used the actual discharge data and the three developed models to estimate net deposition under each condition. These results are provided in Figure 6 and SI Figures S41−S43 of Appendix E-III.

For SS net deposition under the wet year scenario (2003), M_3 shows less cumulative net deposition than the other two models (Figure 6a). Moreover, the upper confidence limit of M_3 (upper red dashed line) is always below the lower confidence limits of M_2 and M_1 (lower blue and green dashed lines), suggesting a statistically significant difference of reservoir performance with the M_3 model. Similar patterns were also observed with the average year (2007) and dry year (2001) scenarios (Figure 6b,c). Not surprisingly, absolute values of cumulative storage increase with wetness of the year, reflecting larger incoming loads for deposition during wet years. (Note the difference of *y*-axis scale among the three panels in Figure 6.) Similar patterns were also observed for TP net deposition modeling (SI Figure S42). Overall, these year-specific comparisons support our major conclusion of decreased net deposition under different hydrological conditions.

DOI: 10.1021/acs.est.5b04073
Environ. Sci. Technol. 2016, 50, 1877−1886

Finally, a note about extreme events—although one may be tempted to similarly reconstruct cumulative storage for the truly wettest years (e.g., 2011, 2004, or 1996 in this record), these years are associated with "extreme flow events" (i.e., TS Lee, Hurricane Ivan, and a major upstream ice-jam release, respectively). For discharges during these extreme flow events, concentration data are relatively sparse and perhaps not fully representative of the range associated with the full history of the events' hydrographs. Statistical modeling has especially high uncertainty in such cases and we therefore avoided these years for the purpose of Figure 6.

4. MANAGEMENT IMPLICATIONS

This paper presents three types of analyses on decadal-scale changes in sediment and nutrient loadings across Conowingo Reservoir on Susquehanna River: $C-Q$ relationships inferred from observed data, loading estimates from standard WRTDS models, and loading estimates from stationary WRTDS models. All three analyses consistently show that average annual net deposition rates of SS and TP have declined in recent years under a wide range of flow conditions that include flows well below the literature-reported scour threshold, with correspondingly increased loads delivered from Susquehanna River to Chesapeake Bay (for any given flow) relative to previous decades. Future progress in Chesapeake Bay restoration will depend on accurate predictions of how inputs of SS, TP, and TN to the reservoirs will be modulated by processes taking place in the reservoirs. Management actions in the Susquehanna River Basin will need to be adjusted to reflect the future role that sediment accumulation and remobilization behind Conowingo Dam will have on the delivery of SS, TP, and TN to the Bay. Our analysis of the evolution of the system to date can help constrain and inform the development and application of improved predictive models of reservoir performance, and particularly the incorporation of such models in the ongoing upgrade of the Chesapeake Bay Partnership's Watershed Model.[5,6] Our results and methods are also applicable to other reservoir systems that may be similarly approaching a state of dynamic equilibrium with respect to sediment storage.

■ ASSOCIATED CONTENT

Supporting Information

The Supporting Information is available free of charge on the ACS Publications website at DOI: 10.1021/acs.est.5b04073.

Appendices A through E are provided (PDF)

■ AUTHOR INFORMATION

Corresponding Author

*Phone: (443) 509-2270; e-mail: qzhang19@jhu.edu.

Notes

The authors declare no competing financial interest.

■ ACKNOWLEDGMENTS

This work was supported by Maryland Sea Grant (NA10OAR4170072 and NA14OAR1470090), Maryland Water Resources Research Center (2015MD329B), National Science Foundation (CBET-1360415), and U.S. Geological Survey Chesapeake Bay Ecosystem Program. We thank Wendy McPherson for providing the photo of Conowingo Dam. We thank Joel Blomquist (USGS), Ken Staver (University of Maryland), and three anonymous reviewers for their constructive comments. Any use of trade, firm, or product names is for descriptive purposes only and does not imply endorsement by the U.S. Government.

■ REFERENCES

(1) Hagy, J. D.; Boynton, W. R.; Keefe, C. W.; Wood, K. V. Hypoxia in Chesapeake Bay, 1950−2001: Long-term change in relation to nutrient loading and river flow. *Estuaries* **2004**, *27* (4), 634−658.

(2) Kemp, W. M.; Boynton, W. R.; Adolf, J. E.; Boesch, D. F.; Boicourt, W. C.; Brush, G.; Cornwell, J. C.; Fisher, T. R.; Glibert, P. M.; Hagy, J. D.; Harding, L. W.; Houde, E. D.; Kimmel, D. G.; Miller, W. D.; Newell, R. I. E.; Roman, M. R.; Smith, E. M.; Stevenson, J. C. Eutrophication of Chesapeake Bay: historical trends and ecological interactions. *Mar. Ecol.: Prog. Ser.* **2005**, *303*, 1−29.

(3) Murphy, R. R.; Kemp, W. M.; Ball, W. P. Long-term trends in Chesapeake Bay seasonal hypoxia, stratification, and nutrient loading. *Estuaries Coasts* **2011**, *34* (6), 1293−1309.

(4) U.S. Environmental Protection Agency. *Chesapeake Bay Total Maximum Daily Load for Nitrogen, Phosphorus and Sediment*; Annapolis, MD, 2010.

(5) Linker, L. C.; Batiuk, R. A.; Shenk, G. W.; Cerco, C. F. Development of the Chesapeake Bay Watershed Total Maximum Daily Load Allocation. *J. Am. Water Resour. Assoc.* **2013**, *49* (5), 986−1006.

(6) Shenk, G. W.; Linker, L. C. Development and Application of the 2010 Chesapeake Bay Watershed Total Maximum Daily Load Model. *J. Am. Water Resour. Assoc.* **2013**, *49* (5), 1042−1056.

(7) Zhang, Q.; Brady, D. C.; Boynton, W.; Ball, W. P. Long-term Trends of Nutrients and Sediment from the Nontidal Chesapeake Watershed: An Assessment of Progress by River and Season. *J. Am. Water Resour. Assoc.* **2015**, *51* (6), 1534−1555.

(8) Langland, M. J. *Sediment transport and capacity change in three reservoirs, Lower Susquehanna River Basin, Pennsylvania and Maryland, 1900−2012*, U.S. Geological Survey Open-File Report 2014-1235; U.S. Geological Survey: Reston, VA, 2015; p 18.

(9) Langland, M. J. *Bathymetry and sediment-storage capacity change in three reservoirs on the Lower Susquehanna River, 1996−2008*, Scientific Investigations Report 2009-5110; U.S. Geological Survey: Reston, VA, 2009; p 21.

(10) Reed, L. A.; Hoffman, S. A. *Sediment Deposition in Lake Clarke, Lake Aldred, and Conowingo Reservoir, Pennsylvania and Maryland, 1910-93*, Water-Resources Investigations Report 96−4048; US Geological Survey: Lemoyne, PA, 1997; p 14.

(11) Friedl, G.; Wüest, A. Disrupting biogeochemical cycles−Consequences of damming. *Aquat. Sci.* **2002**, *64* (1), 55−65.

(12) Jossette, G.; Leporcq, B.; Sanchez, N. Philippon, Biogeochemical mass-balances (C, N, P, Si) in three large reservoirs of the Seine basin (France). *Biogeochemistry* **1999**, *47* (2), 119−146.

(13) Testa, J. M.; Brady, D. C.; Di Toro, D. M.; Boynton, W. R.; Cornwell, J. C.; Kemp, W. M. Sediment flux modeling: Simulating nitrogen, phosphorus, and silica cycles. *Estuarine, Coastal Shelf Sci.* **2013**, *131*, 245−263.

(14) Kemp, W. M.; Sampou, P.; Caffrey, J.; Mayer, M.; Henriksen, K.; Boynton, W. R. Ammonium recycling versus denitrification in Chesapeake Bay sediments. *Limnol. Oceanogr.* **1990**, *35* (7), 1545−1563.

(15) Hainly, R. A.; Reed, L. A.; Flippo, H. N. J.; Barton, G. J. *Deposition and Simulation of Sediment Transport in the Lower Susquehanna River Reservoir System*; U.S. Geological Survey Water-Resources Investigations Report 95-4122; U.S. Geological Survey: Lemoyne, PA, 1995; p 39.

(16) Horowitz, A. J.; Stephens, V. C.; Elrick, K. A.; Smith, J. J. Concentrations and annual fluxes of sediment-associated chemical constituents from conterminous US coastal rivers using bed sediment data. *Hydrol. Process.* **2012**, *26* (7), 1090−1114.

(17) Hirsch, R. M. *Flux of Nitrogen, Phosphorus, and Suspended Sediment from the Susquehanna River Basin to the Chesapeake Bay during Tropical Storm Lee, September 2011, as an indicator of the effects of*

DOI: 10.1021/acs.est.5b04073
Environ. Sci. Technol. 2016, 50, 1877−1886

reservoir sedimentation on water quality, Scientific Investigations Report 2012−5185; U.S. Geological Survey: Reston, VA, 2012; p 17.
(18) Zhang, Q.; Brady, D. C.; Ball, W. P. Long-term seasonal trends of nitrogen, phosphorus, and suspended sediment load from the non-tidal Susquehanna River Basin to Chesapeake Bay. *Sci. Total Environ.* **2013**, *452*−*453*, 208−221.
(19) Langland, M. J.; Hainly, R. A. *Changes in bottom-surface elevations in three reservoirs on the lower Susquehanna River, Pennsylvania and Maryland, following the January 1996 flood - implications for nutrient and sediment loads to Chesapeake Bay*, Water-Resources Investigations Report 97-4138; U.S. Geological Survey: Lemoyne, PA, 1997; p 34.
(20) Gross, M. G.; Karweit, M.; Cronin, W. B.; Schubel, J. R. Suspended sediment discharge of the Susquehanna River to northern Chesapeake Bay, 1966 to 1976. *Estuaries* **1978**, *1* (2), 106−110.
(21) Gellis, A. C.; Hupp, C. R.; Pavich, M. J.; Landwehr, J. M.; Banks, W. S. L.; Hubbard, B. E.; Langland, M. J.; Ritchie, J. C.; Reuter, J. M. *Sources, Transport, and Storage of Sediment at Selected Sites in the Chesapeake Bay Watershed*, Scientific Investigations Report 2008-5186; U.S. Geological Survey: Reston, VA, 2008; p 95.
(22) Brakebill, J. W.; Ator, S. W.; Schwarz, G. E. Sources of suspended-sediment flux in streams of the Chesapeake Bay Watershed: A regional application of the SPARROW model. *J. Am. Water Resour. Assoc.* **2010**, *46* (4), 757−776.
(23) Merritts, D.; Walter, R.; Rahnis, M.; Hartranft, J.; Cox, S.; Gellis, A.; Potter, N.; Hilgartner, W.; Langland, M.; Manion, L.; Lippincott, C.; Siddiqui, S.; Rehman, Z.; Scheid, C.; Kratz, L.; Shilling, A.; Jenschke, M.; Datin, K.; Cranmer, E.; Reed, A.; Matuszewski, D.; Voli, M.; Ohlson, E.; Neugebauer, A.; Ahamed, A.; Neal, C.; Winter, A.; Becker, S. Anthropocene streams and base-level controls from historic dams in the unglaciated mid-Atlantic region, USA. *Philos. Trans. R. Soc., A* **2011**, *369* (1938), 976−1009.
(24) Walter, R. C.; Merritts, D. J. Natural streams and the legacy of water-powered mills. *Science* **2008**, *319* (5861), 299−304.
(25) Massoudieh, A.; Gellis, A.; Banks, W. S.; Wieczorek, M. E. Suspended sediment source apportionment in Chesapeake Bay watershed using Bayesian chemical mass balance receptor modeling. *Hydrol. Process.* **2013**, *27* (24), 3363−3374.
(26) Karl, T. R.; Knight, R. W. Secular Trends of Precipitation Amount, Frequency, and Intensity in the United States. *Bull. Am. Meteorol. Soc.* **1998**, *79* (2), 231−241.
(27) Sprague, L. A.; Langland, M. J.; Yochum, S. E.; Edwards, R. E.; Blomquist, J. D.; Phillips, S. W.; Shenk, G. W.; Preston, S. D. *Factors affecting nutrient trends in major rivers of the Chesapeake Bay Watershed*, Water-Resources Investigations Report 00-4218; U.S. Geological Survey: Richmond, VA, 2000; p 109.
(28) Belval, B. L.; Sprague, L. A. *Monitoring nutrients in the major rivers draining to Chesapeake Bay*, Water-Resources Investigations Report 99-4238; U.S. Geological Survey, 1999; p 8.
(29) U.S. Geological Survey. Surface-water data for the nation. http://dx.doi.org/10.5066/F7P55KJN (accessed 1 June 2014).
(30) Susquehanna River Basin Commission, Sediment and nutrient assessment program. http://www.srbc.net/programs/cbp/nutrientprogram.htm (accessed 1 June 2014).
(31) Hirsch, R. M.; Moyer, D. L.; Archfield, S. A. Weighted regressions on time, discharge, and season (WRTDS), with an application to Chesapeake Bay river inputs. *J. Am. Water Resour. Assoc.* **2010**, *46* (5), 857−880.
(32) Cohn, T. A.; Delong, L. L.; Gilroy, E. J.; Hirsch, R. M.; Wells, D. K. Estimating constituent loads. *Water Resour. Res.* **1989**, *25* (5), 937−942.
(33) Hirsch, R. M. Large Biases in Regression-Based Constituent Flux Estimates: Causes and Diagnostic Tools. *J. Am. Water Resour. Assoc.* **2014**, *50* (6), 1401−1424.
(34) Moyer, D. L.; Hirsch, R. M.; Hyer, K. E. *Comparison of Two Regression-Based Approaches for Determining Nutrient and Sediment Fluxes and Trends in the Chesapeake Bay Watershed*, Scientific Investigations Report 2012−5244; U.S. Geological Survey: Reston, VA, 2012; p 118.
(35) Hirsch, R. M.; De Cicco, L. *User guide to Exploration and Graphics for RivEr Trends (EGRET) and dataRetrieval: R packages for hydrologic data (version 2.0, February 2015)*, Techniques and Methods Book 4, Chapter A10; U.S. Geological Survey: Reston, VA, 2015; p 93.
(36) Helsel, D. R.; Hirsch, R. M. *Statistical Methods in Water Resources*; U.S. Geological Survey: Reston, VA, 2002; p 522.
(37) Hirsch, R. M.; Alexander, R. B.; Smith, R. A. Selection of methods for the detection and estimation of trends in water quality. *Water Resour. Res.* **1991**, *27* (5), 803−813.
(38) Qian, S. S. *Environmental and Ecological Statistics with R*; Chapman and Hall/CRC Press: Boca Raton, FL, 2010.
(39) Hirsch, R. M.; Archfield, S. A.; De Cicco, L. A. A bootstrap method for estimating uncertainty of water quality trends. *Journal of Environmental Modelling and Software* **2015**, *73*, 148−166.
(40) Evans, C.; Davies, T. D. Causes of concentration/discharge hysteresis and its potential as a tool for analysis of episode hydrochemistry. *Water Resour. Res.* **1998**, *34* (1), 129−137.
(41) House, W. A.; Warwick, M. S. Hysteresis of the solute concentration/discharge relationship in rivers during storms. *Water Res.* **1998**, *32* (8), 2279−2290.
(42) Burt, T. P.; Worrall, F.; Howden, N. J. K.; Anderson, M. G. Shifts in discharge-concentration relationships as a small catchment recovers from severe drought. *Hydrol. Process.* **2015**, *29* (4), 498−507.
(43) Richardson, M. C. Contributions of streamflow variability, concentration-discharge shifts and forested wetlands to terrestrial-aquatic solute export in Precambrian Shield headwater catchments. *Ecohydrology* **2012**, *5* (5), 596−612.
(44) Lefrançois, J.; Grimaldi, C.; Gascuel-Odoux, C.; Gilliet, N. Suspended sediment and discharge relationships to identify bank degradation as a main sediment source on small agricultural catchments. *Hydrol. Process.* **2007**, *21* (21), 2923−2933.
(45) Gomez and Sullivan Engineers. *2011 Conowingo Pond Bathymetric Survey, Appendix F of Final Study Report, Sediment Introduction and Transport Study, Conowingo Hydroelectric Project*, 2012; p 129.
(46) The Lower Susquehanna River Watershed Assessment Team, *Lower Susquehanna River Watershed Assessment Phase I Draft Report*; Lower Susquehanna River Watershed Assessment, MD and PA, 2014; p 185.

DOI: 10.1021/acs.est.5b04073
Environ. Sci. Technol. 2016, 50, 1877−1886